



Chan, J. C., Hesse, H. and Wang, P. C. (2023) Wingtip Vortices Characterization with Perspective Upright Correction. In: AIAA AVIATION 2023 Forum, San Diego, CA and Online, 12-16 June 2023, ISBN 9781624107047 (doi: [10.2514/6.2023-4526](https://doi.org/10.2514/6.2023-4526))

There may be differences between this version and the published version. You are advised to consult the published version if you wish to cite from it.

<http://eprints.gla.ac.uk/307573/>

Deposited on 28 September 2023

Enlighten – Research publications by members of the University of Glasgow
<http://eprints.gla.ac.uk>

Experimental Characterization of Wingtip Vortices with Perspective Upright Correction

Jia Cheng Chan¹ and Henrik Hesse²

University of Glasgow Singapore, 537 Clementi Road, Singapore 599493

Peng Cheng Wang³

Singapore Institute of Technology, 10 Dover Drive, Singapore 138683

Accurately predicting wingtip vortices is critical for future development of wake vortex surfing operations. Experimental methods such as wind tunnel tests are the most common and reliable approaches to visualize and characterize the trailing vortices, especially with the advancing Laser Doppler Anemometry (LDA) and Particle Image Velocimetry (PIV) techniques. However, the implementation of LDA or PIV with a single camera to get an upright and perpendicular view angle to the targeted plane can be expensive and time-consuming. To overcome the limitation, this paper proposes a novel methodology for perspective upright correction that allows adjustment of the slanted plane during post-processing. This method can be applied to any visualization effort involving a laser sheet and camera. In this paper the method is demonstrated for the characterization of wingtip vortices for NACA4412 with and without winglets, and the results obtained from the proposed methodology can be used for validation of numerical models to capture the vortex evolution downstream of the wing tips.

I. Introduction

Wake vortex surfing [1, 2] is one of the envisioned solutions to improve aircraft fuel efficiency and reduce the greenhouse gas emissions without making notable changes to the existing aircraft designs. Aircraft with finite wings generate two counter-rotating vortices, with downward flow-field velocity component in-between while the flow-field outboard is moving upward [3]. By flying in the upwash region, the trailing aircraft benefit from higher lift and lesser drag. The concept of vortex surfing is still at the very early stage to be commercialized and operationalized. Although the hardware and software required to realize the operations are attainable, reliability remains a question. A key enabler is the accurate prediction of the vortex behavior and its aerodynamic interactions with the trailing aircraft. Specifically, to determine the optimal position for the trailing aircraft in the formation, it is critical to accurately estimate the development and trajectory of the wingtip vortices generated from the leading aircraft wing and to capture its growth and behavior at the near field.

Wind tunnel testing [4] is an established experimental method for the visualization, characterization, and quantification of wingtip vortices. It is one of the best methods to predict the irregular characteristics of the turbulent flow with a very high confidence level. There are several techniques to experimentally characterize wingtip vortices, including Laser Doppler Velocimetry (LDV) or Anemometry (LDA) and Particle Image Velocimetry (PIV). Despite the differences in technology, all techniques use a similar principle [5]. Smoke, dye, or any other form of particulate

¹ PhD Student, Aerospace Engineering, AIAA Student Member.

² Assistant Professor, Program Director, Aerospace Engineering, AIAA Member.

³ Associate Professor, Engineering Cluster.

is introduced at the inlet of the wind tunnel test section and a laser sheet will illuminate at a plane of interest to visualize the movement of air particles. Different techniques [6-10] are then used to measure and characterize the vortices at the plane.

Sohn and Chang [6] has conducted low-speed wind tunnel experiment using a three-component PIV system to capture the characteristics of the wingtip vortex formation and structure at different angles of attack and wingtip configurations from different camera view angle. Bhagwat et al. [7] utilized a stereoscopic PIV system to measure the aerodynamic loading of a wing under an influence of another wing-vortex wake system. Panagiotou et al. [8] presented a 3D LDA point measurement system to investigate the velocities, vorticity, and circulation quantity of the trailing vortices over different designs of Unmanned Aerial Vehicles (UAVs) at different angles of attack. Most recently, Nagarathinam et al. [9] demonstrated the use of LDV to measure the mean streamwise velocity and the root-mean square of their fluctuations. Various research efforts have shown that wind tunnel testing combined with visual flow measurement techniques can be an effective tool to capture trailing wing vortices.

However, the mentioned systems come at a cost in terms of required time, budget, and infrastructure. Serrano-Aguilera et al. [10] employed a smoke wire technique and introduced a digital camera to analyze the wingtip vortex illuminated by a laser-sheet and captured through the reflections from a tilted mirror behind the wing. The single camera visualization system has greatly reduced the cost compared to LDA or PIV system but the calibration of the camera and tilted mirror in the downstream may be challenging and unattainable for some wind tunnel facilities.

Hence, a novel methodology for perspective upright correction (PUC) is proposed in this paper and demonstrated for experimental wind tunnel results. Section II introduces the new methodology for vortex capturing with smoke particles and shows the wind tunnel setup including the placement of the laser plane and the camera. The paper then presents the post-processing technique of PUC that is able to correct the slanted view of the vortex plane allowing for a single camera to be positioned anywhere in the domain with minimal alignment and calibration efforts. Section III demonstrates the method for a NACA4412 wing and extends the wind tunnel data with numerical results.

II. Methodology

The wind tunnel facility at Singapore Institute of Technology (SIT) [11] , shown in Figure 1, is an open-circuit subsonic suction wind tunnel. It has a test cross-section of 1.2m width, 0.8m height and 2m length [4]. The fan located at the outlet has a diameter of 2m and capable of creating freestream velocities of up to $U_{\infty} = 10m/s$. A pitot tube is placed at the top of the test section midstream to measure the freestream speed. The test section is accessible from the openable panels on both sides. The wind tunnel is also equipped with smoke generator and probe at the test section upstream centerline. The smoke generator probe is adjustable in the vertical z axis.



Figure 1. Wind tunnel at Singapore Institute of Technology.

The workflow overview of the wind tunnel test for vortex visualization is illustrated in Figure 2. There are three main phases namely pre-experiment, vortex capture and post-process.

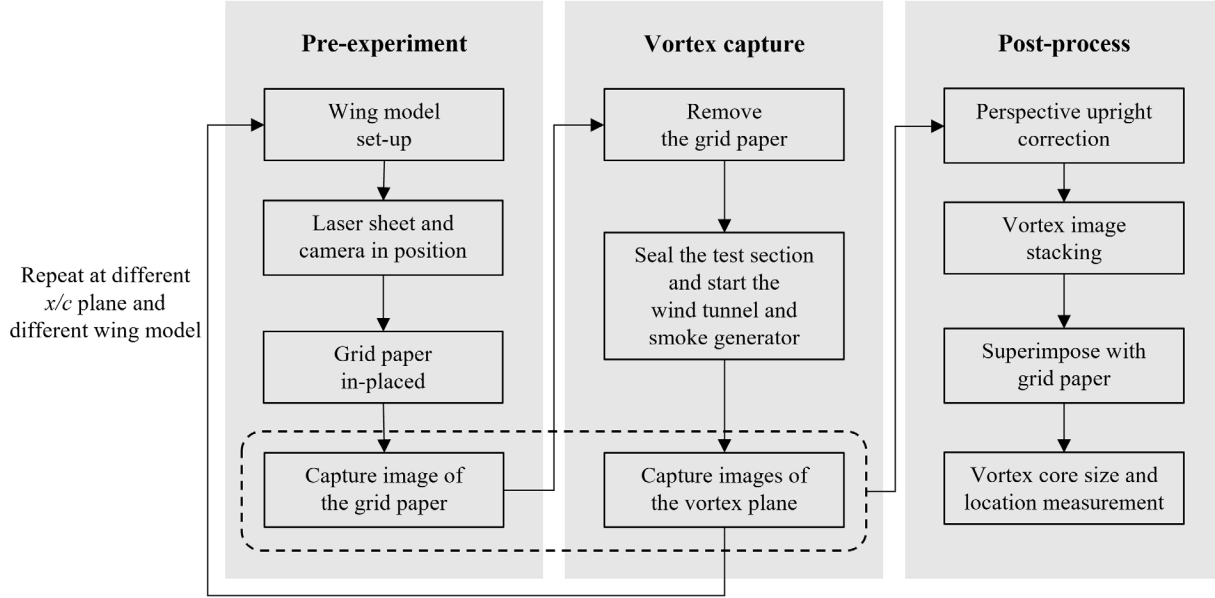


Figure 2. Overview of wind tunnel test workflow.

A. Pre-Experiment

Winglets or wingtip devices [12] have been introduced since the early 20th century to minimize the induced drag. The additional structure reduces the wingtip vortices by preventing the airflow on the pressure surface from slipping to the suction surface. To demonstrate the effect of winglets on the vortex generation, two wing designs are considered: one is a rectangular plain wing without winglet (see Figure 3a) and another one is same wing but with a blended winglet (see Figure 3b).

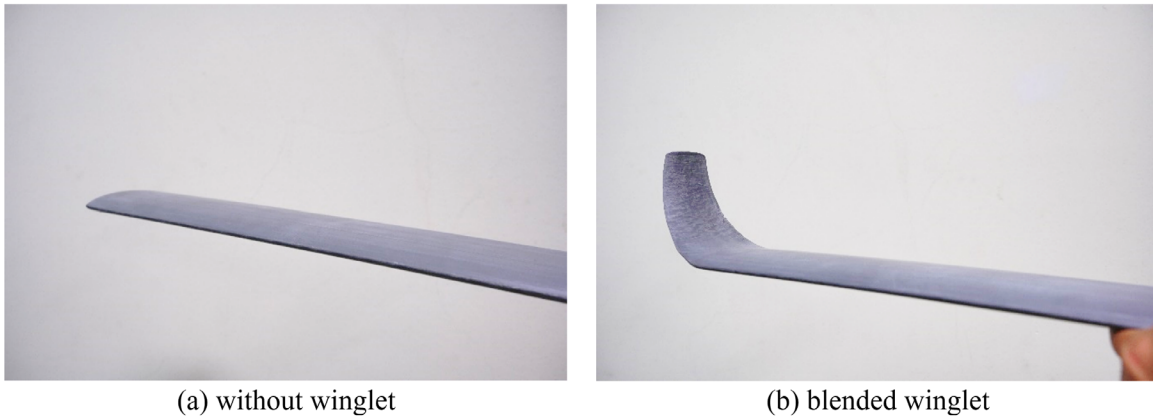


Figure 3. 3D-printed NACA4412 wing model.

1. 3D modelling

The blended winglet design here is swept upwards at the wingtip, with a smooth curvature radius of 0.1m in the transition section and taper ratio of 0.5 at the tip, as shown in Figure 4. Both wings have the same wingspan, and the airfoil profile is the NACA4412 with 0.1m chord length and 0.5m wingspan. Both wing models were 3D-printed with PLA and the surfaces were polished with micro grit sandpaper to achieve a smooth surface finish and minimize the skin friction effect. The Reynolds number based on the chord length of the airfoil for the experiment corresponds to $Re = 6.8 \times 10^4$.

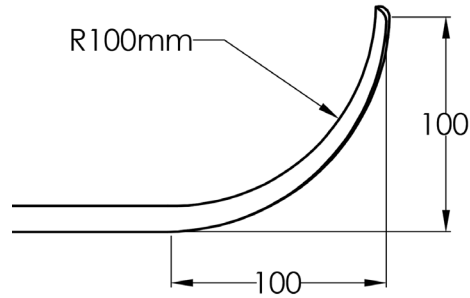


Figure 4. Blended wingtip design with curvature radius = $1c$.

2. Wind tunnel set-up

As shown in Figure 5, the wing model was positioned at the mid height of the test section with a stand, about $x/c = 5$ downstream to the smoke probe. The wingtip is aligned to the centerline with the smoke particle probe. In this work, a laser sheet emitter with a 2.5mm grid width [13] is used to illuminate the smoke particles. To visualize the wake vortices, the continuous green-color laser sheet is positioned at various y - z planes from $x/c = 0$ to $x/c = 10$ with the aid of x/c indicator labelled at the bottom of the test section. A 24-megapixel, mirrorless camera [14] with variable focal length of 28-70mm and maximum aperture of f -stops 2.8 [15] is placed $x/c = 8$ in the downstream of the laser sheet emitter. The tunnel blockage effect is negligible as the blockage area by the camera is less than 0.85%.

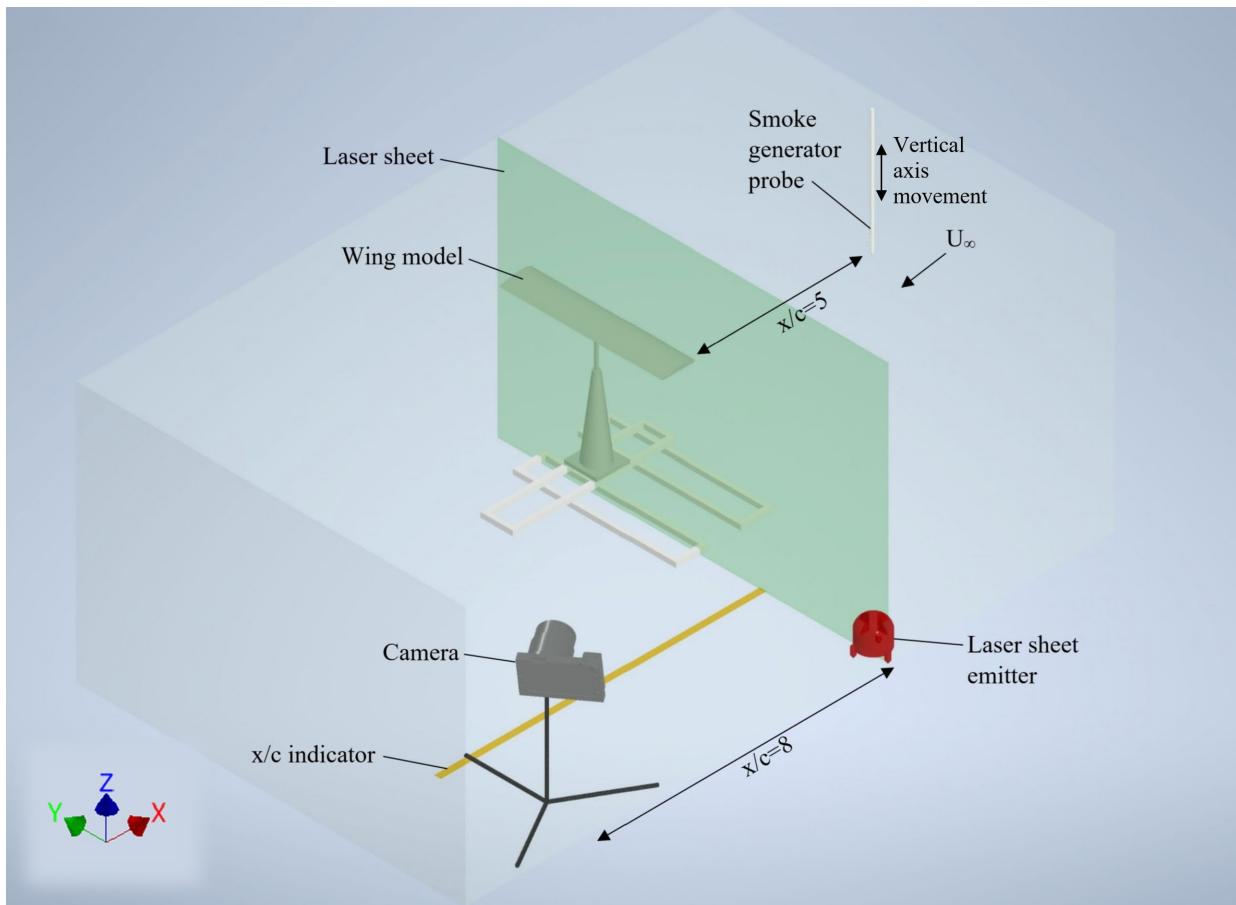


Figure 5. Overview of the wind tunnel experiment for vortex visualization.

3. Problem identification

In order to capture the vortex pattern accurately, the viewing angle of the camera needs to be perpendicular to the laser-plane. However, it was found that the smoke particles will cover up the camera view and hence lose visibility to the vortex pattern. The camera position was then shifted to the outboard side of the wind tunnel to have a clearer view to the vortex plane. As the viewing angle is now compromised due to the position shift, there is a need for further calibration to ensure that the camera can capture the vortex plane perpendicularly. Thus, a sheet of 5mm x 5mm grid with circles origin at the center of the grid (see Figure 6a) was printed and placed at the laser sheet plane which is normal to the freestream airflow direction and the center of the grid is aligned with the wingtip trailing edge as shown in Figure 6b.

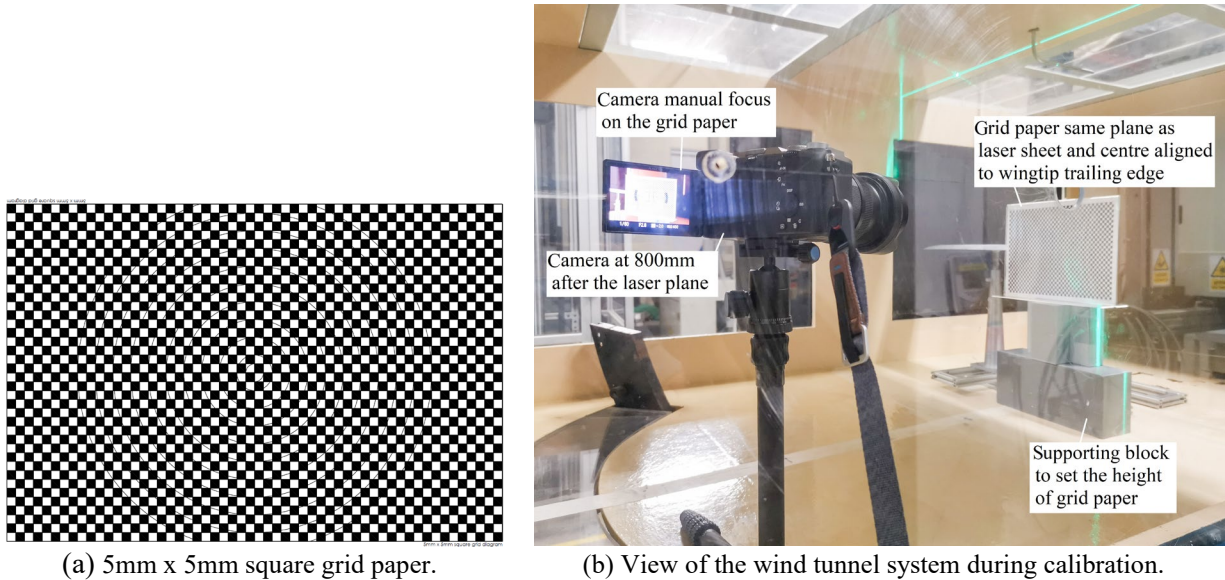
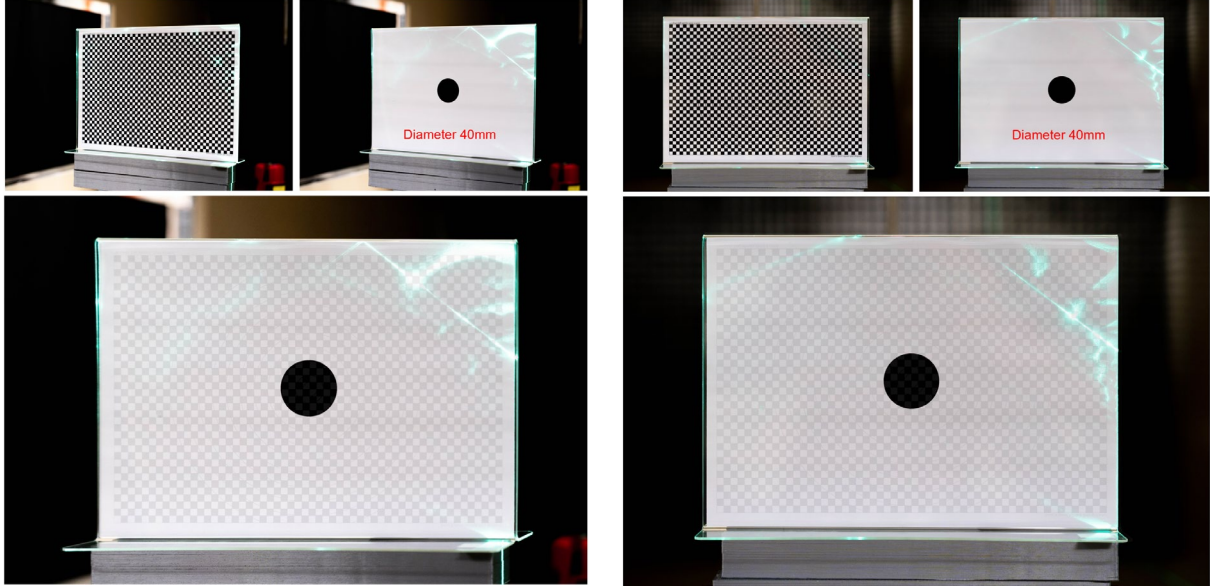


Figure 6. Wind tunnel system during calibration of the vortex plan.

The camera mounted on the tripod is adjusted to the same height as the wing and pointed at the grid paper. The camera setting for the wind tunnel test is ISO640, shutter speed of 1/250s or faster, aperture $f/2.8$, zoom focal length of 70mm and manual focus to the center of the grid paper. The setting is to provide sharp, focused images on the vortices, with adequate light intensity and acceptable level of noise. An image of the grid paper is taken as the calibration baseline before removing it and activating the wind tunnel and smoke probe.

4. Validation test

Before starting the experiment on the wing model, a separate validation test has been carried out to examine the accuracy of the proposed perspective upright correction (PUC) versus the native upright view. Both methods capture the same grid paper and a printed solid black circle of diameter 40mm, at different view respectively. The images in both cases are post-processed and superimposed, as shown in **Error! Reference source not found.**, and measurements are carried out with a digitizer tool [16] for validation purpose. Remarkably, the result of employing the PUC has fared better than the native upright view, with -0.5225% to +0.1565% of inaccuracy compared to -0.6696% to +0.8379%. The negligible error is believed to be the sensitivity error, but not caused by the correction. This has proven the PUC is a valid approach to process a slanted view of plane and producing an accurate result as compared to native upright view,



(a) Perspective upright correction.

(b) Native upright view.

Figure 7. Validation of perspective upright correction accuracy.

B. Vortex Capture

The same laser implementation and camera setting are used to capture the vortex at the exact location where the grid paper was placed during calibration. The laboratory lighting is turned off during the experiment to produce a higher contrast image on the vortex without over-exposing the area highlighted with laser.

One limitation encountered in the experiment is that the smoke stream formed by the smoke generator probe is concentrated in a small area, and in some cases, it is smaller than the vortex size. Hence, the smoke probe is moved in the vertical z -axis to capture the vortex pattern outside the initial smoke stream. Multiple photos of the vortices are taken as the smoke probe is moving in the vertical direction, to provide more information on the vortex structures outside of the initial smoke probe area on the laser plane. Figure 8 shows examples of how the different areas of the vortex can be captured. The multiple photos are post-processed and stacked together with the baseline photo of the grid paper. The superimposed image allows measurement of the vortex core size, flow structure and location.

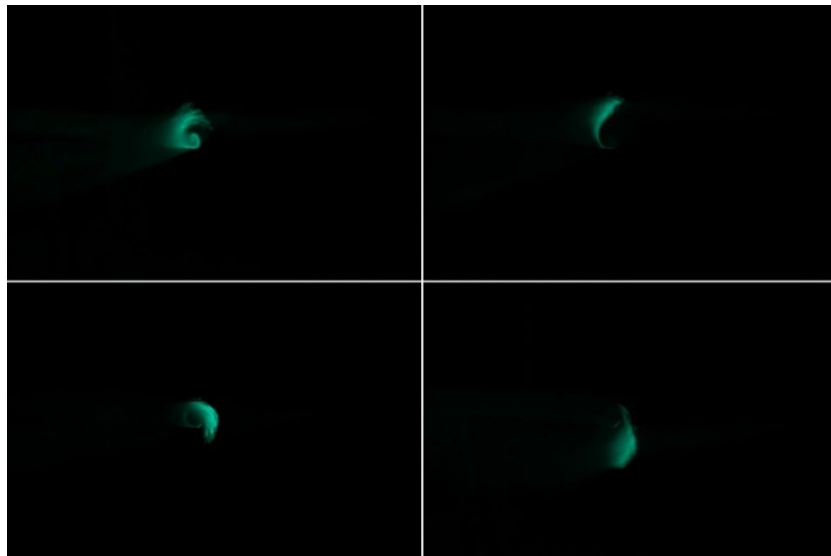


Figure 8. Examples of vortices captured for wing without winglet ($\alpha = 12^\circ$, $x/c = 0$), before PUC.

To capture the vortex propagation in the streamwise direction, the experiment can be repeated by shifting the laser sheet emitter and camera together in the downstream x/c direction, up to $x/c=10$. The alignment of grid paper and the setting of camera are then re-initialized before the image capturing of grid paper and vortices. After the series of images are taken at the various x/c positions, the test is then repeated for different angles of attack α and wing models.

C. Post-Process

As the camera is pointed at the vortex plane at an angle, the results are tilted and slanted from the upright viewing angle, as shown in Figure 9a. To rectify this problem, a post-processing of perspective upright correction (PUC) is necessary to make the computation of vortex core size, location, and flow structure possible. In this initial study, the photos taken in the wind tunnel are imported to Adobe Lightroom Classic [17] for post-processing. In each case setup, the photo of grid paper is processed first with the PUC in guided mode, which allows the user to draw up to four lines as the vertical and horizontal guide. To minimize the error in the rectification, the guided line is drawn on the outer most grid boundary, as illustrated in Figure 9b. The image is now set in an upright position with the guided lines. Next, a cropping is needed to enlarge the grid paper to fill up the frame of the image, as shown in Figure 9c. There is also lens profile correction feature in the software, for correcting the camera lens distortion and vignetting. After all the adjustment, the grid paper is now facing normal to the viewing angle and upright in horizontal as well as vertical, as shown in Figure 9.

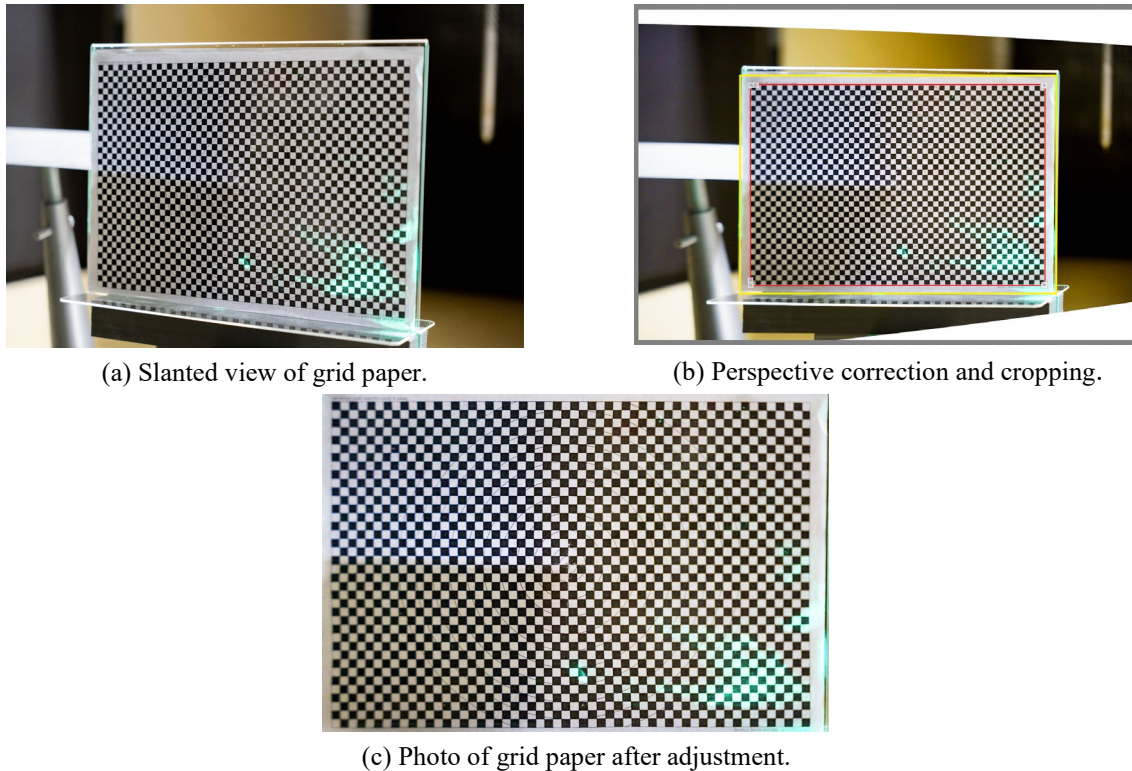


Figure 9. Perspective upright correction and cropping in Adobe Lightroom.

The correction made on the pixel position and geometry of the grid paper is replicated and batch applied to the rest of the vortex photos taken in the same case study. Figure 10 shows examples of the corrected view of vortex after applying the PUC on Figure 8.

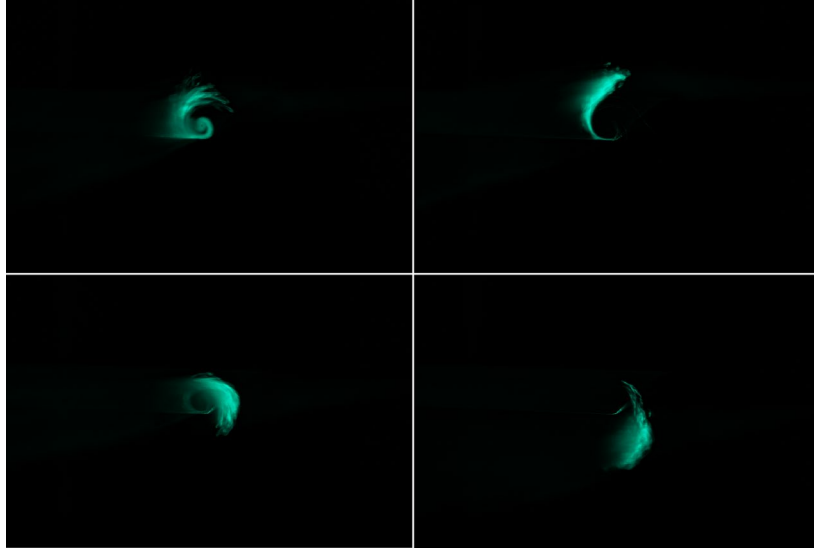


Figure 10. Same vortices from Figure 8 for wing without winglet ($\alpha = 12^\circ$, $x/c = 0$), after PUC.

The group of upright corrected pictures are then imported to Adobe Photoshop [18] to combine all photos and form the full picture of the vortex. At the layer palette in Photoshop, the blending mode of every photo is changed to lighten mode. The software will look at the pixel color information in the layered photos and select the lighter or brighter color to blend into the base photo. Those pixels in the previous layer with darker color than the blend color will be replaced, while the lighter pixels will remain unchanged. The effect of lighten layering or stacking is shown in Figure 11.

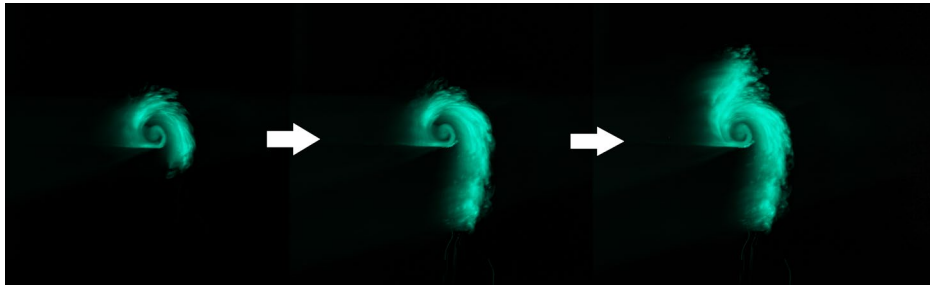


Figure 11. Layer stacking of vortex images with Lighten Blend Mode in Adobe Photoshop.

To capture the entire vortex in detail, up to 30 photos are blended for each x/c location. In the same project file, the grid paper image is finally superimposed over the resulting vortex image with 5% opacity (see Figure 12). This grid paper layer enables the measurement of vortex core size and location as discussed in Section III.


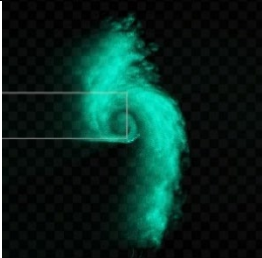
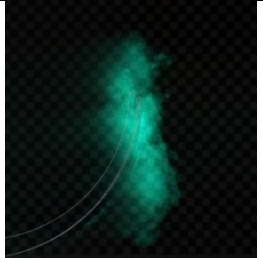
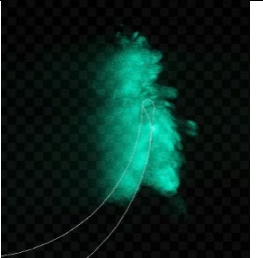
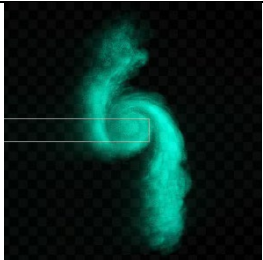
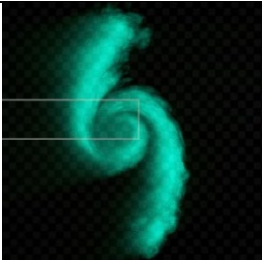
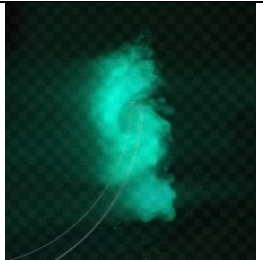
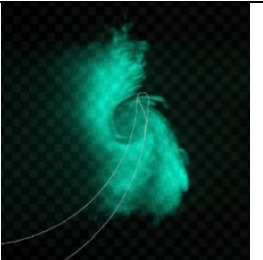
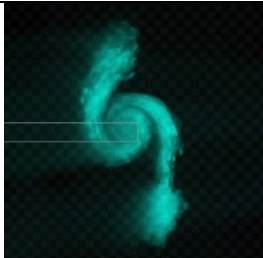

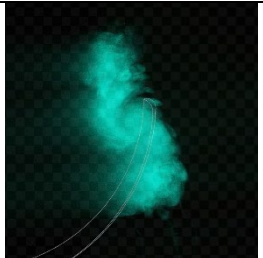
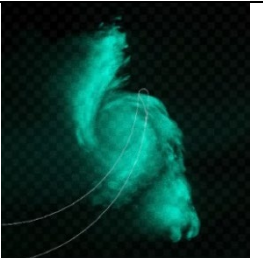

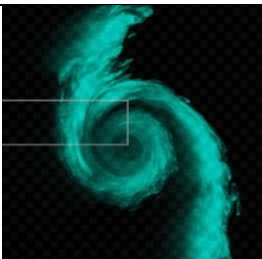
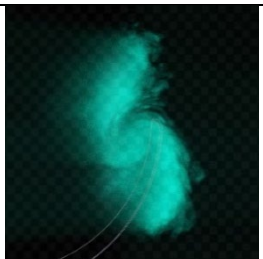
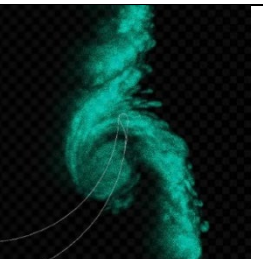
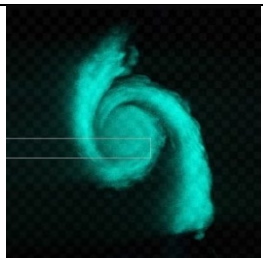
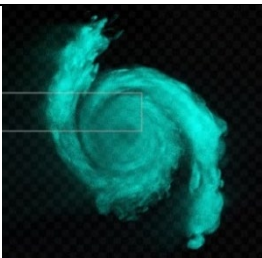
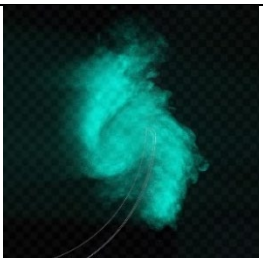
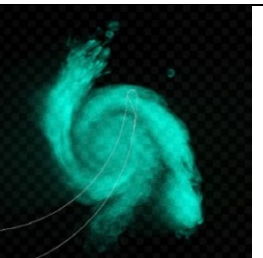


Figure 12. Final vortex image superimposed with grid paper and wing profile.

III.Results

The proposed methodology to capture wing vortices has been exercised on the NACA4412 wing – one without winglet and one with blended winglet, at angles of attack of 2° and 12° . The post-processed images are tabulated in Table 1, it can be clearly seen that the vortex shed from the plain wing is more pronounced, and the vortex core can be identified more easily, compared to the wing with blended winglet, which serves its purpose to reduce the vortex size. This is very similar to Sohn and Chang's work [6], where the presence of winglets helped to reduce the wingtip vortices and its associated induced drag.

Table 1. Vortices captured for NACA4412 rectangular wing without winglet.

x/c	No winglet		Blended winglet	
	$\alpha = 2^\circ$	$\alpha = 12^\circ$	$\alpha = 2^\circ$	$\alpha = 12^\circ$
0				
1				
2				
3				
4				

To characterize and quantify the wing vortices we aim to analyze the vortex size. Devenport et al. [19] defined the contour of the wake spiral as the locus of peak axial turbulence stress, which describes the shape of the vortex core. The same model has been used in other studies of wingtip vortices conducted using wind tunnel facilities with a hot wire technique [6, 8, 10]. The wake spiral in this experiment is not clearly defined since a smoke probe is used instead of the hot wire. However, the structure of the vortex core is still traceable via the smoke streaks bounded by the darker contour in the image.

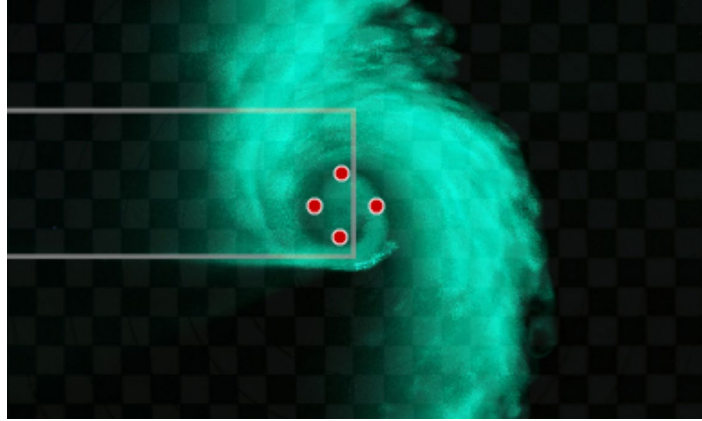


Figure 13. Plotting of quadrant points of vortex core.

As shown in Figure 13, a digitizer tool [16] is used to plot the four quadrant points (red dots) of the wake spiral of the vortex core, to compute the center of the vortex core and the radius in y and z direction. However, there is still missing information on the vortex profile such as the tangential velocity U_θ , which is of significant for wake vortex surfing application. Hence, the following Lamb-Oseen model [20, 21] is used to estimate the U_θ of the vortex at each x/c downstream location:

$$U_\theta = \frac{\Gamma_V}{2\pi r} \left[1 - e^{-1.26 \left(\frac{r^2}{r_c^2} \right)} \right] \quad (1)$$

where r_c is the characteristic radius of the vortex core measured from the plotted quadrant points, and r is the radial distance of any point (y, z) from the vortex core center (y_0, z_0) ,

$$r = \sqrt{(y - y_0)^2 + (z - z_0)^2} \quad (2)$$

and Γ_V is the circulation of the vortex at each x/c plane calculated using the Kutta Joukowski's theorem [22] as:

$$\Gamma_V = \frac{L_G}{\rho U_\infty b_V} \quad (3)$$

where L_G is typically the weight of the vortices generating aircraft, but for the wind tunnel test here, it represents the lift generated on the wing. As there is no force balance instrument or pressure sensor implemented in the experiment, the lift force of the plain rectangular wing is estimated by referring to other studies [23, 24, 25] on the aerodynamics performance of NACA4412 wing with similar aspect ratio and Reynolds number. The approximated C_L for $\alpha=2^\circ$ and 12° is 0.549155 and 1.099364 respectively. The lift of the blended winglet is assumed to be about 8.4% higher than the wing without winglet, according to the experimental outcomes presented by Ara et al. [25]. U_∞ is the freestream velocity and b_V is the span between the counter-rotating pair of vortices, which can be calculated from the shifting of the vortex core position.

From the experiments and literatures, it is noticed that the blended winglet has generally higher lift coefficient under the same condition, and smaller vortex core radius by 45% and 31% at $\alpha = 2^\circ$ and 12° respectively. These has resulted in a higher tangential velocity in the Lamb-Oseen model as shown in Figure 14. The graphs are plotted with origin at the vortex core and showing the profile of U_θ across the radius of the wingtip vortices at different x/c plane.

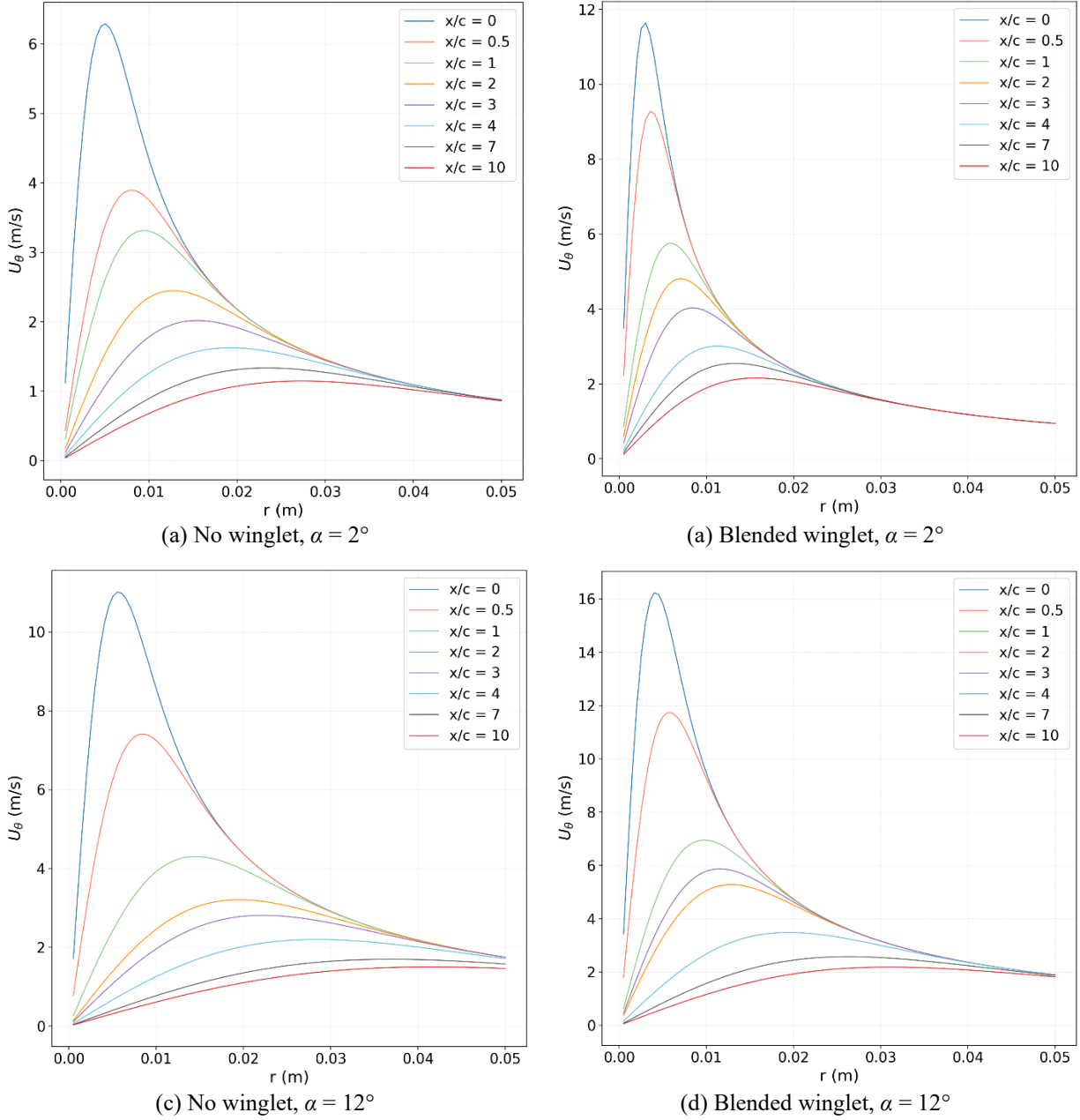
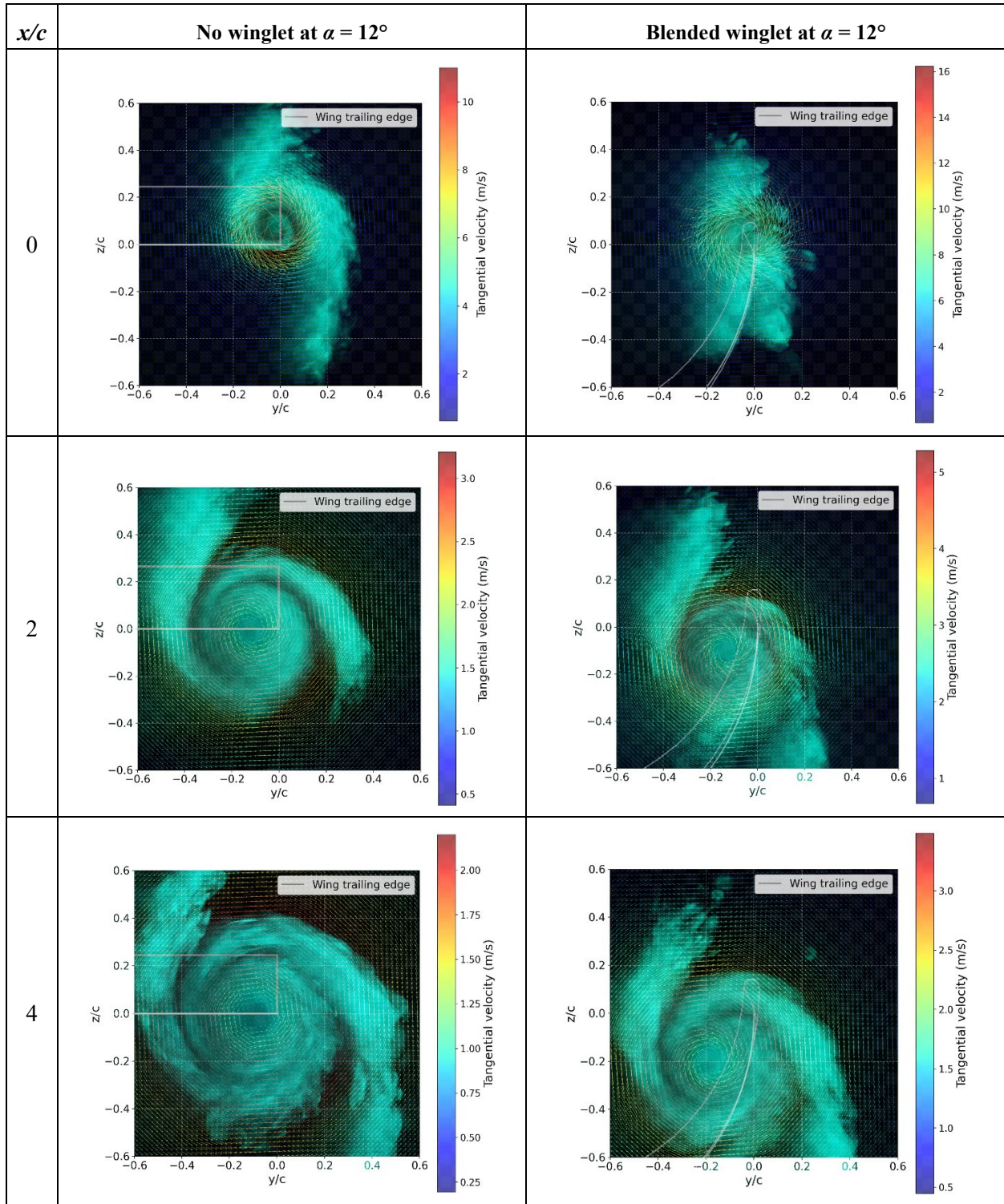


Figure 14. Tangential velocity profile across core radius.

To visualize the flow field better, the Lamb Oseen tangential velocity vector field is plotted on the image of the vortices in Table 2, for both wing models at $\alpha=12^\circ$ and at plane $x/c = 0, 2$ and 4 , to provide the additional information on the tangential velocity profile of the vortices. Given that the vortex core radius is extracted from the images, the results has matched up nicely with the pattern of the vortices, with core region of higher tangential velocity and peaked at the circumference of the core diameter, then a surrounding region of decreasing velocity as the distance to the vortex core increases.

Table 2. Lamb Oseen vortex model on $\alpha=12^\circ$, $x/c = 0, 1, 2$ and 3 .



For each vortex core, the core location with respect to the wingtip trailing edge and size of core radius were computed and plotted in Figure 15, Figure 16 and Figure 17 to visualize the overview of the vortex core trajectory and the vortex size development.

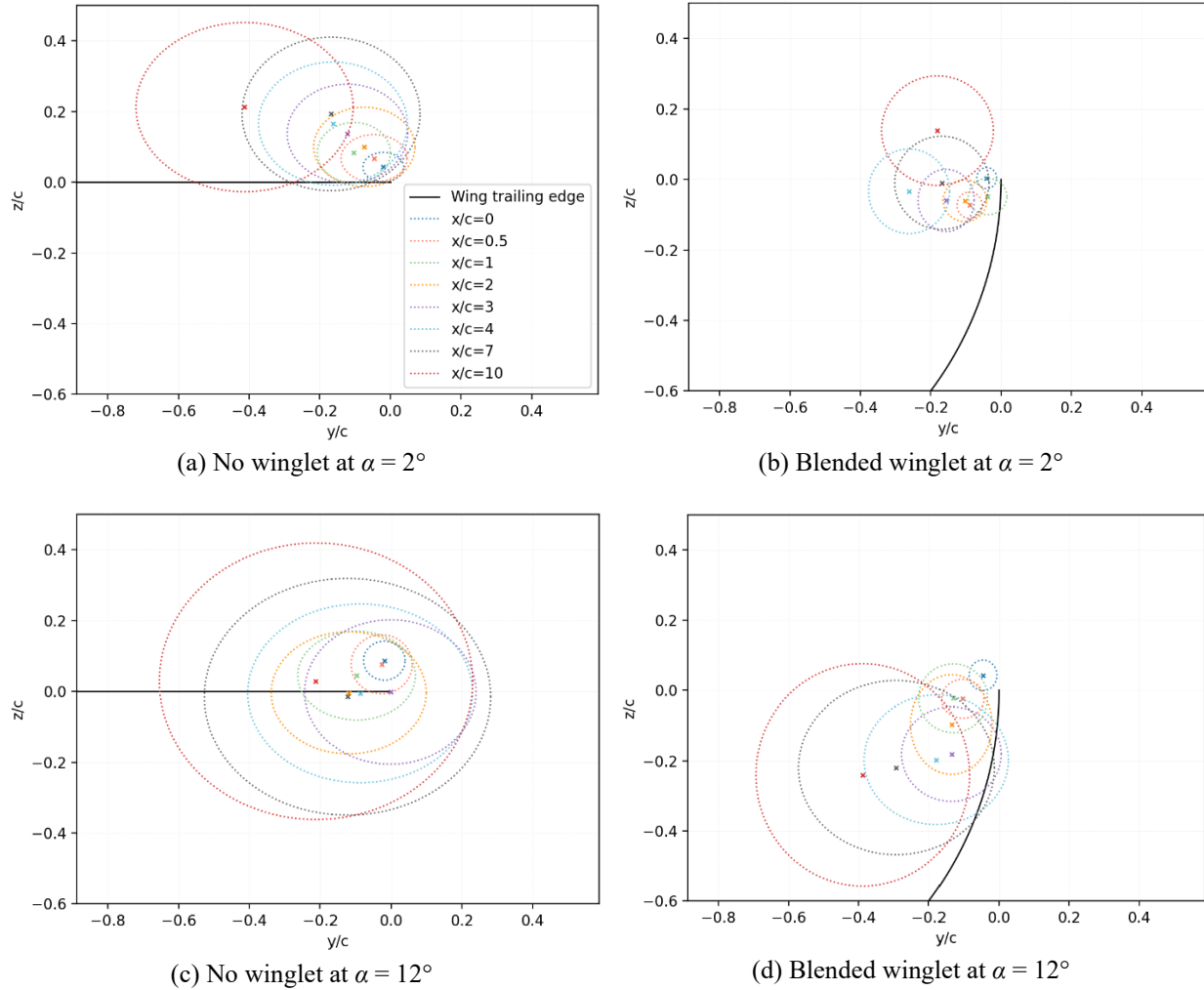
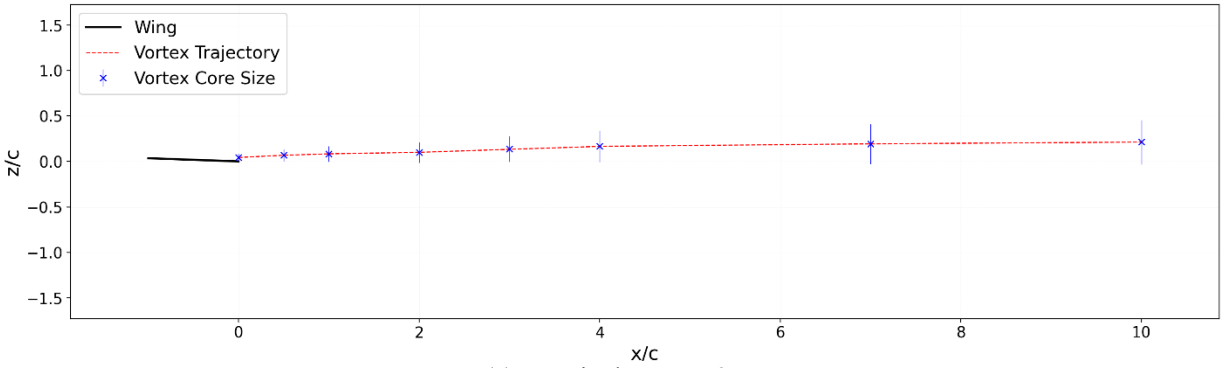


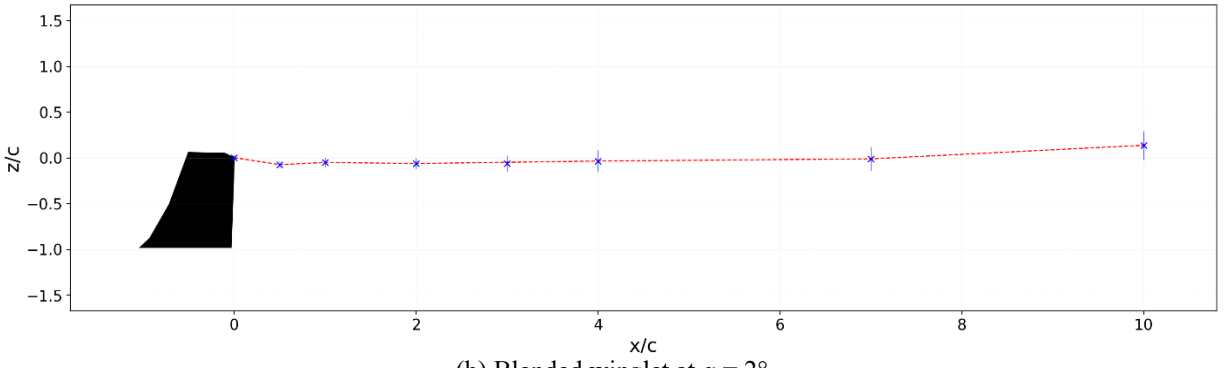
Figure 15. Overview of the vortex cores development, rear view.

From Figure 15 and Figure 17, it is observed that the trailing vortices have moved towards the wing root direction, and this inboard shift is ranged between $-0.2c$ to $-0.4c$, as airflow going downstream from $x/c=0$ to $x/c=10$. The result agrees with O'Regan et al. [26], and it has confirmed that the airflow over the pressure surface tends to roll in toward the fuselage over the wingtip trailing edge which consequently causes the vortex to deviate laterally at a rate that decreases with distance downstream [19].

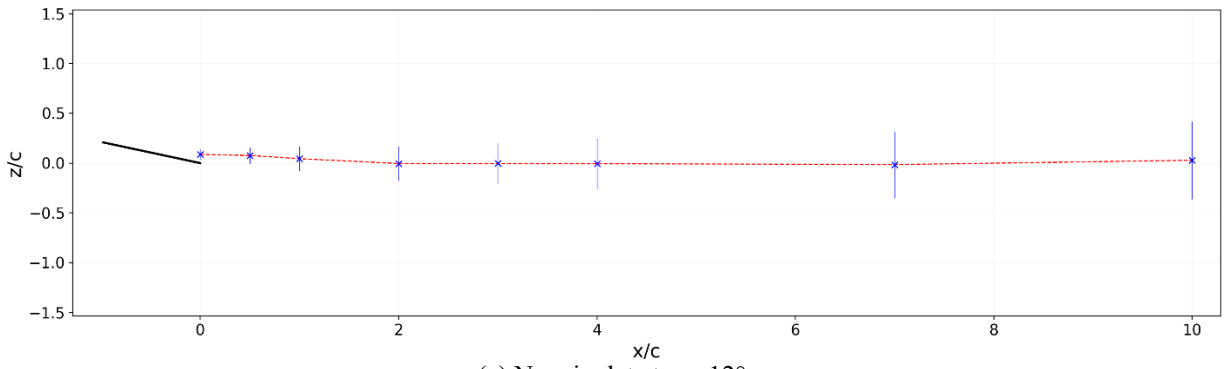
When looking at vertical shift of the vortex core in Figure 15 and Figure 16, an interesting phenomenon is noticed. For both wing designs, either with or without winglet, the vortices induced from the $\alpha = 2^\circ$ and $\alpha = 12^\circ$ have opposite behavior in terms of the horizontal direction. At $\alpha = 2^\circ$, the vortex core is travelling upwards, while the vortex core is going downwards for the case of $\alpha = 12^\circ$. It is hypothesized that the greater lift generated at a higher α , produces a more pronounced wingtip vortex, and induced downward velocity which projects the airflow downwards [3].



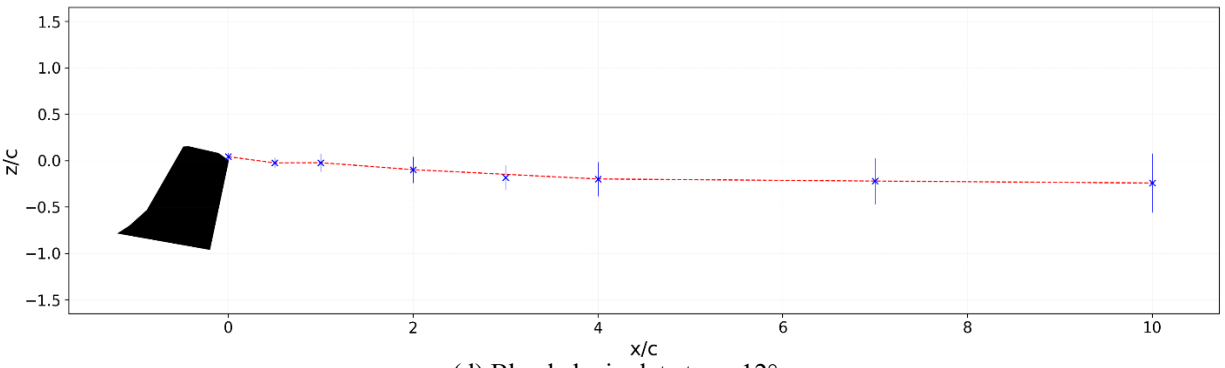
(a) No winglet at $\alpha = 2^\circ$



(b) Blended winglet at $\alpha = 2^\circ$

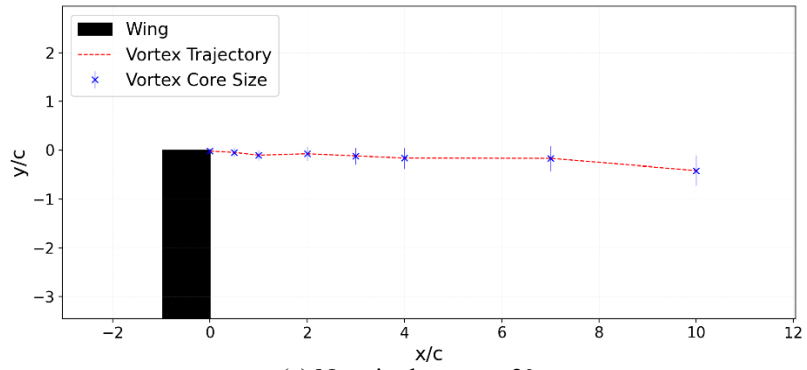


(c) No winglet at $\alpha = 12^\circ$

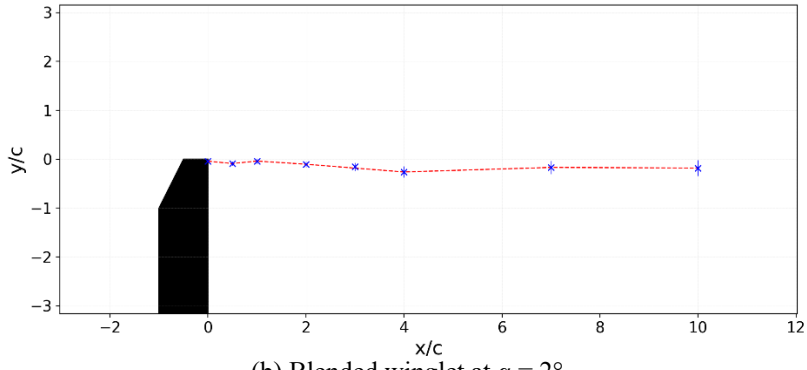


(d) Blended winglet at $\alpha = 12^\circ$

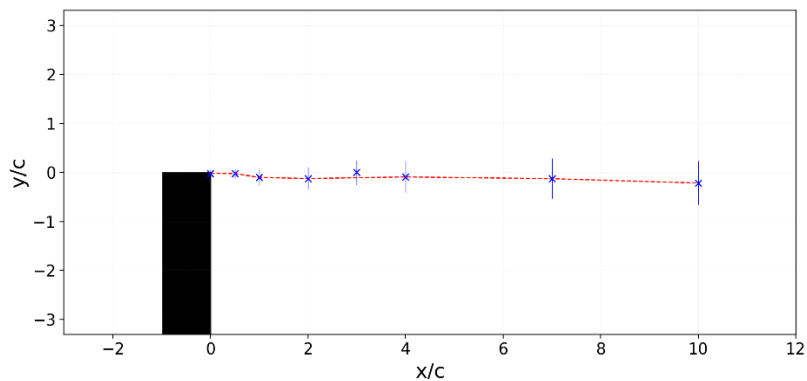
Figure 16. Vortex trajectory and development, side view.



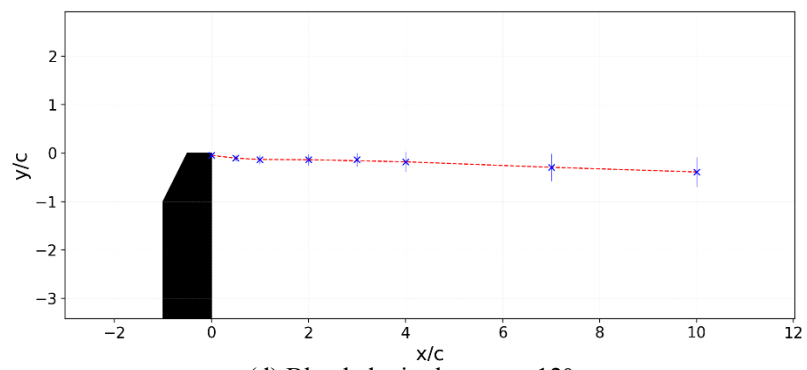
(a) No winglet at $\alpha = 2^\circ$



(b) Blended winglet at $\alpha = 2^\circ$



(c) No winglet at $\alpha = 12^\circ$



(d) Blended winglet at $\alpha = 12^\circ$

Figure 17. Vortex trajectory and development, top view.

IV. Conclusion

This paper has introduced a new, cost-effective method to capture wing wake vortices in wind tunnel experiments. The proposed perspective upright correction (PUC) method provides a simple way to capture and characterize vortices from a single camera with a tilted slanted viewing angle. It allows the camera to be mounted and positioned at any possible location as long as the grid paper for initialization can be captured within its view. The simple validation test has proved that the accuracy of the image capturing and processing for the slanted view image is comparable with or better than the native upright camera view. Moreover, the wind tunnel test with the PUC performed was demonstrated on a wing model with blended winglets to show the reduction of the core size of the wingtip vortices typical for such winglet configurations.

The vortex core radius and location are then used to model the vortex physics using Lamb Oseen vortex model. Despite the limitations of the numerical model such as the axisymmetric vortex assumption and uniform vortex core shape and size, the result of each x/c plane has shown the growth of vortex size with decaying tangential velocity. The information may provide some guidelines on the vortices encountered by the trailing aircraft in the wake vortex surfing.

The proposed methodology can be further improved for any future work on wind tunnel experiment. The laser sheet emitter and camera may be placed outside of the wind tunnel to keep the wind tunnel test section clean. The processing for image correction may be automated using existing computer vision approaches. The methodology can also be implemented with Particle Image Velocimetry (PIV) to capture the velocities and obtain both quantitative and qualitative results of the complex flow behavior downstream of bluff bodies.

Acknowledgments

The work is part of the Industrial Postgraduate Program co-funded by the Economic Development Board of Singapore and ST Engineering Aerospace Ltd. The author would also like to acknowledge Jeremy Wong (Aircraft Systems Engineering, SIT, Class of 2023), for his contribution in the design and 3D print of the airfoils.

References

- [1] Y. Zhao, H. Wu, Q. Zhang and Q. Cheng, "Overview of surfing aircraft vortices for energy," *Journal of Physics: Conference Series (The 11th Asia Conference on Mechanical and Aerospace Engineering ACMAE)*, vol. 1786, no. 1, pp. 12-26, 2021.
- [2] W. B. Blake, S. R. Bieniawski and T. C. Flanzer, "Surfing aircraft vortices for energy," *The Journal of Defense Modeling and Simulation: Applications, Methodology, Technology*, vol. 12, no. 1, pp. 31-39, 2013.
- [3] C. Breitsamter, "Wake vortex characteristics of transport aircraft," *Progress in Aerospace Sciences*, vol. 47, no. 2, pp. 89-134, 2011.
- [4] Y. S. Lim, P. C. Wang, J. J. Yeo and S. C. M. Yu, "Experimental and numerical studies for flow over a sierpinski tetrahedron for potential windbreak application," *Journal of Wind Engineering & Industrial Aerodynamics*, vol. 216, 2021.
- [5] B. Chanetz, J. Détery, P. Gilliéron, P. Gnemmi, E. R. Gowree and P. Perrier, *Experimental Aerodynamics An Introductory Guide*, Cham, Switzerland: Springer, 2020.
- [6] M. H. Sohn and J. W. Chang, "Visualization and PIV study of wing-tip vortices for three different tip configurations," *Aerospace Science and Technology*, vol. 16, pp. 40-46, 2012.
- [7] M. J. Bhagwat, F. X. Caradonna and M. Ramasamy, "Wing-vortex interaction: unraveling the flowfield of a hovering rotor," *Experiments in Fluids*, vol. 1, p. 56, 2015.
- [8] P. Panagiotou, G. Ioannidis, I. Tzivinikos and K. Yakinthos, "Experimental Investigation of the Wake and the Wingtip Vortices of a UAV Model," *Aerospace*, vol. 4, no. 53, 2017.

- [9] D. Nagarathinam, J.-W. Hong, B.-K. Ahn, C. Park, G.-D. Kim and I.-S. Moon, "Dynamics of tip vortex flow over three dimensional hydrofoils by LDV measurements," *Ocean Engineering*, vol. 266, no. 1, 2022.
- [10] J. J. Serrano-Aguilera, J. H. García-Ortiz and A. Gallardo-Claros, "Experimental characterization of wingtip vortices in the near field using smoke flow visualizations," *Exp Fluids*, vol. 57, no. 137, 2016.
- [11] "Singapore Institute of Technology," [Online]. Available: <https://www.singaporetech.edu.sg/>.
- [12] D. McLean, "Wingtip Devices: What They Do and How They Do It," in *Performance and Flight Operations Engineering Conference*, Seattle, WA, 2005.
- [13] "Aiguru Laser Level Green Line 4B1H Comes With Remote | Model : LASER-AGR-LD5150-4B1H," Aik Chin Hin Hardware & Machinery, 2022. [Online]. Available: <https://www.aikchinhin.sg/products/aiguru-laser-level-green-line-4b1h-c-w-remote-model-laser-agr-ld5150-4b1h>.
- [14] "Interchangeable-lens Cameras | Alpha 7C Compact full-frame camera | ILCE-7C/ILCE-7CL," Sony, 2022. [Online]. Available: https://www.sony.com.sg/interchangeable-lens-cameras/products/ilce-7c?locale=en_SG&cpint=HOMEPAGE_TOPBANNER_DIILCE7C_8524.
- [15] "28-70mm F2.8 DG DN | Contemporary," Sigma, 2022. [Online]. Available: https://www.sigma-global.com/en/lenses/c021_28_70_28/.
- [16] A. Rohatgi, "WebPlotDigitizer v4.6," [Online]. Available: <https://apps.automeris.io/wpd/>.
- [17] "Adobe Lightroom Classic," Adobe, 2022. [Online]. Available: <https://www.adobe.com/sg/products/photoshop-lightroom.html>.
- [18] "Adobe Photoshop," Adobe, 2022. [Online]. Available: <https://www.adobe.com/sg/products/photoshop.html>.
- [19] W. J. Devenport, M. C. Rife, S. I. Liapis and G. J. Follin, "The structure and development of a wing-tip vortex," *Journal of Fluid Mechanics*, vol. 312, pp. 67-106, 1996.
- [20] F. Holzapfel, T. Gerz, M. Frech and A. Dornbrack, "Wake Vortices in Convective Boundary Layer and Their Influence on Following Aircraft," *Journal of Aircraft*, vol. 37, no. 6, pp. 1001-1007, 2000.
- [21] N. N. Ahmad, F. H. Proctor, F. M. L. Duparcmeur and D. Jacob, "Review of Idealized Aircraft Wake Vortex Models," in *AIAA SciTech 52nd Aerospace Sciences Meeting*, National Harbour, Maryland, 2014.
- [22] H. Hesse and R. Palacios, "Dynamic Load Alleviation in Wake Vortex Encounters," *Journal of Guidance, Control, and Dynamics*, vol. 39, no. 4, pp. 801-813, 2016.
- [23] M. N. Haque, M. Ali and I. Ara, "Enhancing aerodynamic performance of NACA 4412 aircraft wing using leading edge modification," in *6th BSME International Conference on Thermal Engineering (ICTE 2014)*, 2015.
- [24] D. S. Körpe, Ö. Ö. Kanat and T. Oktay, "The Effects of Initial γ plus: Numerical Analysis of 3D NACA 4412 Wing Using γ -Re θ SST Turbulence Model," *European Journal of Science and Technology*, no. 17, pp. 692-702, 2019.
- [25] I. Ara, M. Ali, M. Q. Islam and M. N. Akhter, "An Experimental Investigation on the Aerodynamic Characteristics of NACA 4412 with Winglets," in *AIP Conference Proceedings 2121*, 2019.
- [26] M. S. O'Regan, P. C. Griffin and T. M. Young, "A vorticity confinement model applied to URANS and LES simulations of a wing-tip vortex in the near-field," *Journal of Heat and Fluid Flow*, vol. 61, pp. 355-365, 2016.